

DETECTING THE ONSET OF NUCLEATE BOILING IN INTERNAL COMBUSTION ENGINES

Teresa Castiglione¹, Francesco Pizzonia¹, Rocco Piccione¹ and Sergio Bova^{1*}

¹DIMEG, Department of Mechanical, Energy and Management Engineering,
Università della Calabria, Via P. Bucci, Cubo 44C, 87036 Rende, ITALY

*Corresponding author: tel. +39 0984 494828, email address: sergio.bova@unical.it

ABSTRACT

The use of an electric pump instead of the standard crankshaft-driven one in Internal Combustion Engines, gives the possibility of controlling the coolant flow rate independently of engine speed, allowing therefore, the use of much lower coolant flow rates than usually adopted and the development of nucleate boiling flow regimes within the engine cooling system. In order to take advantage of nucleate boiling and of the associated high heat transfer coefficients, the onset of this heat transfer regime must be correctly identified. This work presents the results of an experimental campaign, which was carried out on a small displacement spark ignition engine (1.2 dm³, 60 kW) with the aim of detecting the occurrence of nucleate boiling within the engine cooling system. The test rig was properly instrumented in order to measure coolant temperatures at engine inlet and outlet, coolant pressure at several locations in the circuit, coolant flow rate and engine metal temperatures. Operating conditions involving different coolant flow rates were selected in order to enforce both the usual single-phase heat transfer regime and nucleate boiling conditions. Several experimental quantities were analyzed with the aim of establishing the coolant flow rates ranges where the nucleate boiling occurs. The agreement in the trend of coolant temperature and pressure and engine wall temperature provides hints to identify experimentally the onset of nucleate boiling.

32

HIGHLIGHTS

33

- Cooling system of an internal combustion engines equipped with an electric pump.

34

- Onset of Nucleate Boiling experimentally detected by coolant flow rate regulation.

35

- Different experimental techniques tested.

36

- Effects of coolant pressure on Nucleate Boiling Onset investigated.

37

38

KEYWORDS

39

Nucleate boiling; thermal management; cooling system; experimental test; electric pump;

40

internal combustion engines.

41

42

43 1. INTRODUCTION

44 Thermal management plays an important role for Internal Combustion Engines (ICE)
45 performances, emissions, fuel consumption and reliability. Nowadays many works deal, in
46 particular, with the behavior of the cooling system during the engine warm-up. As is known,
47 in fact, high engine emissions and fuel consumption occur at low engine temperatures owing
48 to high frictional losses and combustion inefficiency. Will et al. [1,2] estimated an increase in
49 frictional losses amounting to 2.5 times the ones obtained under fully warmed conditions, for
50 lubricant temperatures around 20°C, while engine efficiency drops to about 9% after a cold
51 start [1,3]; Samhaber et al. [4] predicted an increase of about 13.5% in fuel consumption for
52 lubricant temperatures around 0 °C. A fast warm-up is therefore desirable and can be
53 achieved by an optimal thermal management control strategy.

54 The control of the engine cooling system today is still very simple and the possibility of
55 regulation is limited: the rotational speed of the cooling pump is imposed by the engine speed
56 and the cooling system is designed to ensure engine reliability by providing adequate coolant
57 flow rate under high-power conditions. Under low-load or low coolant temperature
58 conditions, the coolant flow direction is managed by using a wax thermostatic valve, which
59 by-passes the radiator and redirects part of the coolant to the pump, while the coolant flow
60 rate is regulated by varying the flow resistance that is determined by the thermostatic valve.
61 In most engine operating conditions, therefore, the coolant flow rate is higher than strictly
62 necessary and the coolant is maintained in liquid phase. Brace [5], for instance, estimated that
63 an engine is over-cooled for 95% of its operating time.

64 Different cooling management strategies were proposed in order to overcome the
65 standard cooling system limitations and most of them are based on the possibility of using an
66 electric pump, whose speed can be controlled independently of engine speed. Ap and Golm
67 [6] proposed a reduction of the coolant flow rates by the use of a small electric water pump.
68 Brace [5,7] proposed the use of an electric pump in cooperation with a throttle valve and
69 developed a control strategy based on the use of empirical look-up tables; 2% improvement
70 in bsfc was obtained. Bent [8] proposed a cooling strategy where the pump was switched on
71 and off cyclically, in order to obtain a faster warm-up, while Gardiner [9] investigated the
72 effects of coolant circulation rate on fuel consumption reduction during engine warm-up.

73 Regulation of coolant flow rates by means of electrically driven pumps, in conjunction
74 with a proper control strategy, can be conveniently used to allow the cooling system to

75 operate under controlled nucleate boiling flow regime [10,11], both during engine warm-up
76 and under fully warmed conditions. The possibility of adopting new components for the
77 cooling system of internal combustion engines and of taking advantage of the nucleate
78 boiling regime was investigated by several researchers for decades [12-16] and is still under
79 investigation [17]; these contribute to identify the advantages of operating under nucleate
80 boiling: smaller coolant mass, smaller radiator, lower pump power requirements, faster
81 warm-up time, and lower friction during the warm-up period; all these conditions allow the
82 reduction of fuel consumption and, consequently, of CO₂ emissions [18], which is currently
83 sought by these and other advanced internal combustion engine technologies [19,20]. In
84 addition, a coolant pump working independently of the engine would eliminate the risk of
85 unwanted phenomena, like after-boiling [21]. Recently, Pizzonia et al. [22] proposed and
86 developed a control strategy which sets the coolant flow rate at much lower values than
87 usually adopted, allowing a certain level of nucleate boiling. Under fully warmed conditions,
88 a coolant flow rate just below that which determines nucleate boiling, ensures appropriate
89 cooling with low coolant flow rate, still preserving engine reliability.

90 However, at present, the difficulty of obtaining on-board information about the heat
91 transfer regime, which occurs under the various operating conditions, is the main obstacle to
92 setting up a practical nucleate boiling cooling system. In order to overcome this limitation
93 and to enable the development of such an innovative system, a deeper understanding of the
94 behavior of a cooling system as a result of the different operating conditions is needed. At the
95 moment, no systematic experimental analysis of Onset of Nucleate Boiling (ONB) in ICE
96 exists.

97 The present work summarizes the results of an extensive experimental campaign, which
98 was carried out at the engine test-rig, with a Spark Ignition (SI) engine properly instrumented,
99 with the purpose to detect the occurrence of nucleate boiling and to identify the engine
100 variables which cause nucleate boiling. Although the test rig is well instrumented, the
101 experimental identification of nucleate boiling is not simple: the observation of vapor bubbles
102 through transparent windows placed along the cooling circuit is not reliable, owing to the fact
103 that in the early stages of nucleate boiling bubbles form but implode before arriving at the
104 window; they become visible only in the fully developed stage of the phenomenon.
105 Therefore, several experimental techniques to identify the Onset of Nucleate Boiling have
106 been developed and are summarized in the present paper. A zero-dimensional model of the
107 cooling system of an SI Engine, which was developed in [10] and is able to predict

108 dynamically the occurrence and the extent of nucleate boiling flow regime, was used to help
109 to explain better the recorded data.

110 **2. EXPERIMENTAL SETUP**

111 The experimental tests were carried out on a small-size four-stroke SI engine. The
112 engine displaces about 1.2 dm³ in four in-line cylinders with four-valve per cylinder
113 aluminum head and about 60 kW between 5000 and 6000 rpm rated power. The standard
114 crankshaft-driven coolant pump is substituted by a small power electric pump (127 W at 15
115 V, 2092 dm³/h maximum flow rate). A schematic of the test-rig is plotted in Figure 1.

116 Special attention was dedicated to the cooling circuit instrumentation (Fig. 2). A
117 differential pressure gauge is installed at the pump ends, while the coolant pressures at engine
118 inlet and outlet are measured with miniature piezoresistive pressure transducers, 3 kHz
119 bandwidth. PT100-type temperature sensors are used to obtain the coolant temperatures at
120 engine inlet and outlet. Coolant volumetric flow rate is measured at engine inlet and outlet
121 using turbine type flowmeters, with a repeatability of $\pm 0.05\%$. In addition, an optical access
122 is also installed in the cooling circuit near the engine outlet, in order to observe the presence
123 of bubbles in the coolant flow pattern during the experimental tests (Fig. 1). The standard
124 radiator is immersed in a tank filled with water, which also contains the coolant expansion
125 tank. A digital PID regulator is used to control the cool water flow rate, which is needed in
126 the tank in order to keep engine inlet coolant temperature constant (85 °C) within a ± 1 °C
127 error band. Finally, k-type thermocouples are located in the cylinder block (head gasket side)
128 and in the cylinder head at various locations, as reported in Figure 3. The main measuring
129 devices specifications are reported in Table 1.

130 All tests are performed with a 50/50 (by mass) mixture of water and commercially
131 available ethylene glycol.

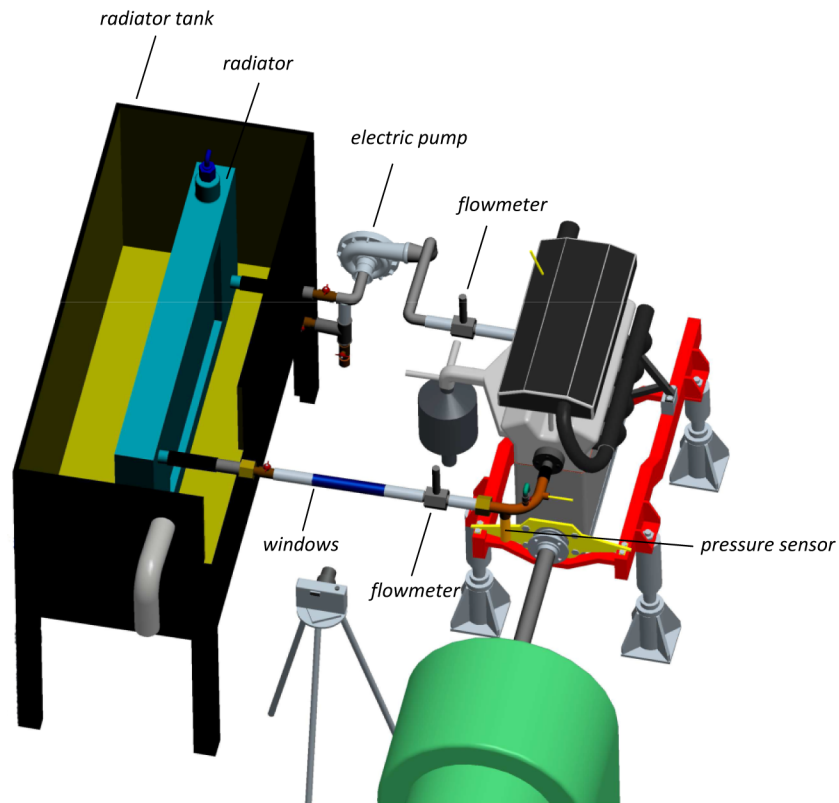


Fig. 1. Schematic of the test rig.

132

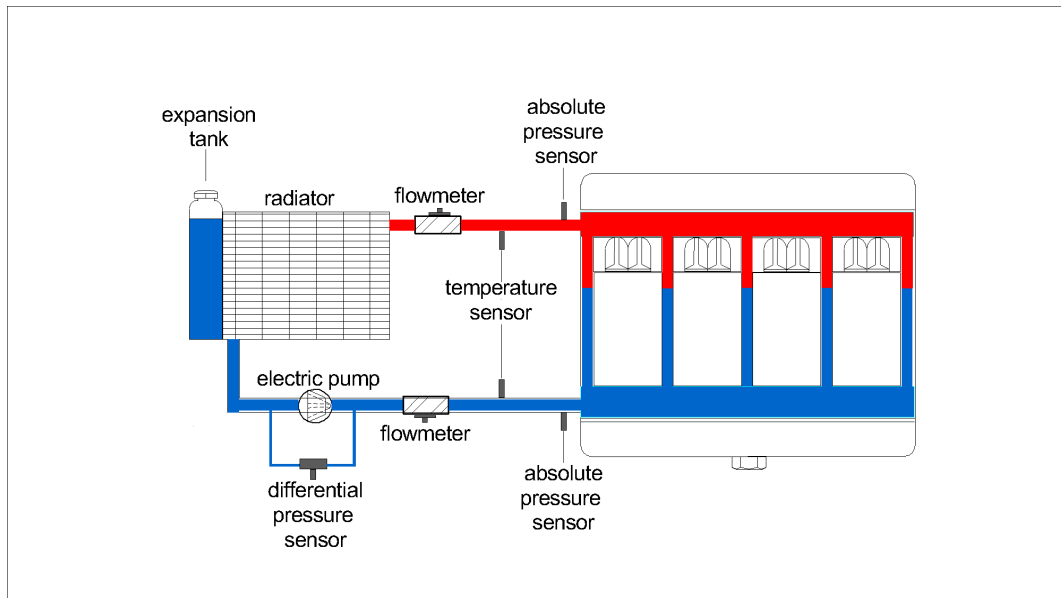


Fig. 2. Schematic of the cooling circuit.

133

134

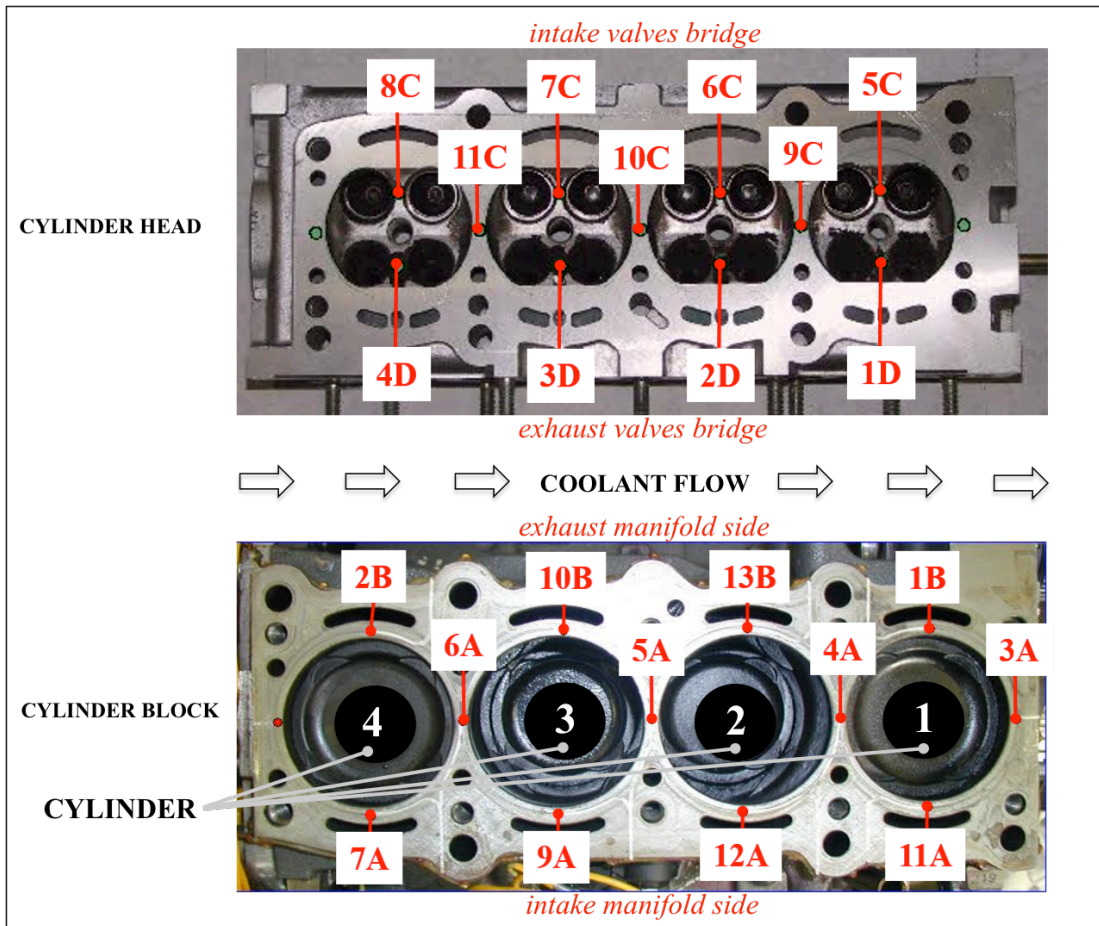


Fig. 3. Thermocouples location in the engine metal and cylinder number identification.

Table 1
Main measurement devices specifications.

Device type	Model	Specifications
AVL, fuel meter	733 S	FS 150 kg/h Sensitivity and linearity deviation $\pm 0.12\%$ of the fuel mass withdrawn
BORGHI&SAVERI, eddy current dynamometer	FE 260 S	FS 190 kW @ 12000 rpm Speed measurement: FS 20000 rpm, resolution 1 revolution, accuracy \pm revolution Torque measurement: FS 2000 Nm, resolution 1 digit, accuracy $\pm 0.1\%$ FS
EG&G FLOW TECHNOLOGY, flow meter	FT-12	FS 75 l/min Repeatability $\pm 0.05\%$ of reading Linearity $\pm 0.5\%$ over normal
EG&G FLOW TECHNOLOGY, flow meter	FT-16	FS 190 l/min Repeatability $\pm 0.05\%$ of reading Linearity $\pm 0.5\%$ over normal
Pt100 temperature sensor	TRC#P1A1X	FS 120 °C Precision ± 0.15 °C
K-type thermocouples		FS 1000 °C Precision ± 1.5 °C
KULITE, pressure sensor	ETQ-12-375	FS 10 bar Resolution infinitesimal Bandwidth 3kHz

135

136 **2.1 Experimental activity**

137 Specific experimental tests were carried out to understand better the behavior of the
138 cooling circuit. First of all, the effects of temperature on coolant pressure were investigated.
139 The coolant pressure was measured within the sealed cooling circuit for different coolant
140 temperatures going from 15°C to 80°C, while both engine and pump were switched-off.
141 Subsequently, the pump head was recorded at switched off engine and coolant temperature of
142 about 15°C. During the tests, the pump voltage was fixed and the coolant flow rate in the
143 circuit was varied through a gate valve. The circuit characteristic was also measured: in such
144 case, the gate valve was left completely open and the coolant flow rate was varied by varying

145 the pump speed. Finally, in order to identify the onset of nucleate boiling several
 146 experimental campaigns were carried out, with different couples of engine speed – bmep
 147 values, both under steady state and transient conditions. Here, a specific test is reported,
 148 where the engine was operated under stable conditions at fixed engine speed (2000 rpm) and
 149 bmep (2 bar), while the coolant flow rate was varied from a maximum value of 2000 dm³/h
 150 down to 500 dm³/h as a sequence of steady state conditions. The coolant temperature at the
 151 engine inlet was kept constant at 85± 1°C. Tests were replicated on different days to assess
 152 the day-by-day repeatability [10]. The experimental tests are summarized in Table 2.

153
 154
 155

Table 2
 Summary of the experimental tests.

Goal	Coolant Temperature	Operating conditions
Coolant thermal expansion analysis	15-85 °C	Engine off/pump off
Pump internal characteristic quantification	15°C	Engine off/ fixed pump speed, gate valve regulation
Circuit characteristic quantification	15°C	Engine off/ wide open gate valve, pump speed regulation
ONB detection	85°C	2000 rpm 2 bar bmep; 2000 to 500 dm ³ /h flow rate

156 3. RESULTS

157 The analysis of the experimental data was focused on three main physical quantities:
 158 coolant pressure, coolant temperature and metal temperature. Other quantities like the coolant
 159 pressure pulsations or the engine-in/engine-out volumetric flow rate comparison, which
 160 proved useful for detecting the onset of the nucleate boiling in [11], where an atmospheric
 161 expansion tank was used, are not presented here. In the presence of a standard closed radiator
 162 expansion tank their indications are, in fact, not clear enough.

163
 164
 165
 166

167 **3.1 Coolant pressure**

168 Coolant pressure not only gives useful information regarding the presence of nucleate
169 boiling, but also directly and strongly influences its onset. Coolant pressure is determined by
170 two main contributions.

171 First, it is determined by coolant expansion caused by temperature increase. In fact, as
172 the coolant volume increases while the total volume of the circuit is fixed, the air volume
173 within the expansion tank (Fig. 2) decreases and the circuit pressure increases. Figure 4
174 presents two sets of experimental data of coolant pressure vs. coolant average temperature
175 (symbols), which were collected on different days, and which were obtained by keeping both
176 the engine and coolant pump off. The experimental data show a linear trend in the 60-85 °C
177 range of temperature. Data, however, differ considerably day-by-day even though the coolant
178 level within the cooling system was kept constant; this is due to the temperature of the water
179 within the radiator tank (Fig. 1), which controls coolant engine inlet temperature, and is
180 therefore not constant. This affects the air temperature within the radiator expansion tank
181 (Fig. 2) and consequently its pressure. Out of this arises a warning on the repeatability of the
182 nucleate boiling phenomenon in the engine under real operating conditions. A difference in
183 the initial coolant level within the cooling circuit or an air leakage of the radiator cap (a
184 component costing few euro) would cause a significant discrepancy in the operating pressure
185 of the cooling circuit and consequently an important variation in the tendency to the onset of
186 nucleate boiling.

187 A second contribution to coolant pressure is determined by the pump head. The pump
188 speed increases with voltage and, for any fixed voltage, the pump head decreases as the flow
189 rate increases. Figure 5 shows the characteristic of the pump at 13V and the pressure-flow
190 rate characteristic of the hydraulic circuit. It is interesting to observe that, as the circuit is
191 sealed, the pump action develops partly by determining an increase in the absolute pressure at
192 the delivery side and for the remaining part by determining a decrease in the pressure at the
193 suction side. This second contribution can be even greater than the first one and changes as
194 the coolant temperature varies (Fig. 6).

195 During the tests for ONB detection (Table 2 row 4), the coolant temperature was
196 measured; the coolant pressure was then estimated by adding the contribution due to the
197 thermal expansion, which results from this temperature on the basis of Fig. 4 correlation, to
198 the contribution due to pump head. Pump head variations due to the fluid temperature
199 increase would only provide a second order correction. The results are presented in Figure 7.

200 The effect of coolant expansion is computed in the two different situations of Figure 4. This
201 determines a variation of 0.4-0.5 bar in the coolant total pressure of Figure 7. However, the
202 trend is similar in both cases and this pressure rises as the coolant flow rate increases. In
203 Figure 8, this calculated total coolant pressure has been made equal to the experimental
204 pressure at engine inlet in the range of coolant flow rate 1400-1700 dm³/h and compared with
205 the experimental value of coolant pressure measured at engine inlet and engine outlet as a
206 function of coolant flow rate.

207 Independently of the absolute values, it is evident that the trend is the same for coolant
208 flow rates higher than 1200-1300 dm³/h, where the heat transfer regime is that of single-
209 phase forced convection. For lower coolant flow rates, the measured engine-in and engine-out
210 pressure increases as the coolant flow rate diminishes and the reason is the onset of nucleate
211 boiling within the cooling circuit. In fact, the presence of bubbles makes the coolant thermal
212 expansion greater than the one due to temperature increase only. This difference in pressure
213 trend can therefore be used as an indication of the onset of nucleate boiling. For coolant flow
214 rates of about 1200-1300, however, bubbles are not yet visible at the transparent window, as
215 they condense and collapse within the bulk flow short after they form; their presence can be
216 noted for much lower flow rates, about 950-1050 dm³/h. As the coolant flow rate further
217 diminishes the fully developed sub-cooled boiling condition establishes at a value of about
218 950 dm³/h, where the bulk liquid temperature reaches the saturation temperature (saturated
219 boiling), and a net vapor production is visible at the transparent window (*FBD*). These two
220 flow rates values are indicated by the two vertical dashed lines in Fig. 8, where a few pictures
221 of the coolant, taken through the transparent window, are also presented.

222

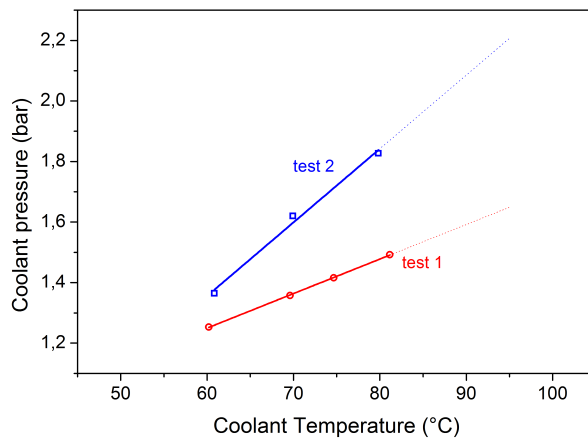


Fig. 4 Influence of the coolant temperature on coolant pressure within the sealed circuit at switched-off engine and pump.

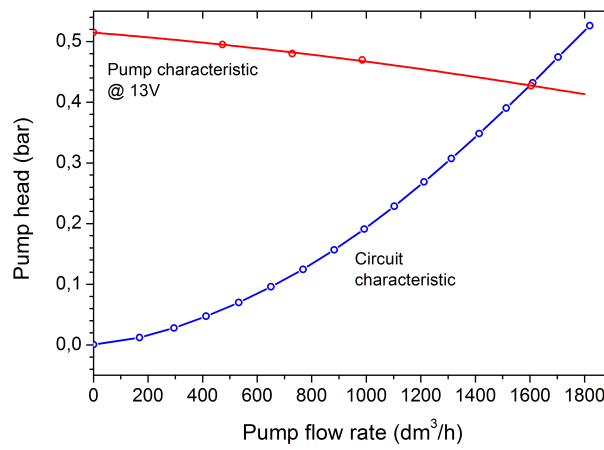


Fig. 5 Pump and circuit characteristics.

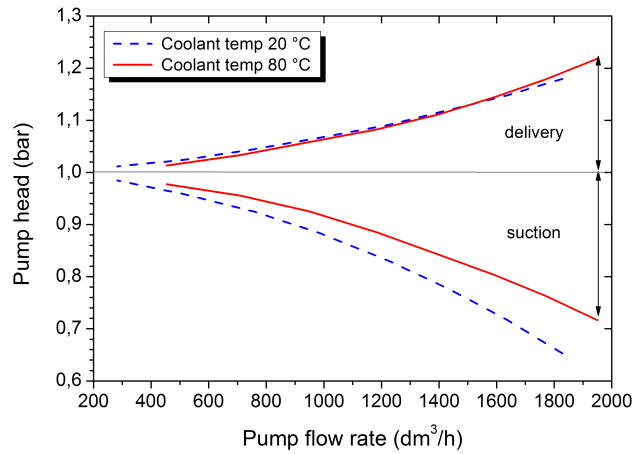


Fig. 6 Fractions of pump head which develops at pump delivery and at pump suction side.

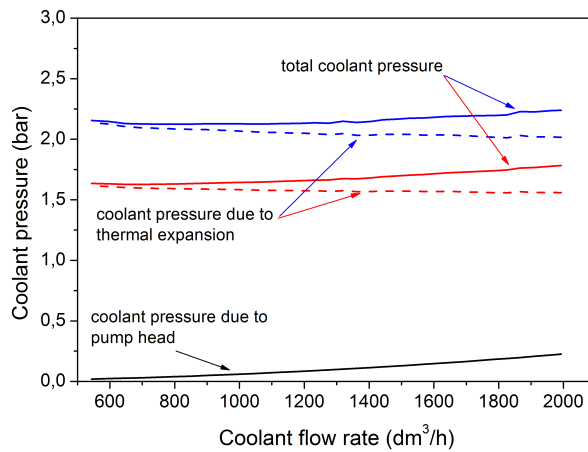


Fig. 7 Coolant pressure owing to the sum of coolant expansion and pump head contributions as a function of volumetric coolant flow rate.

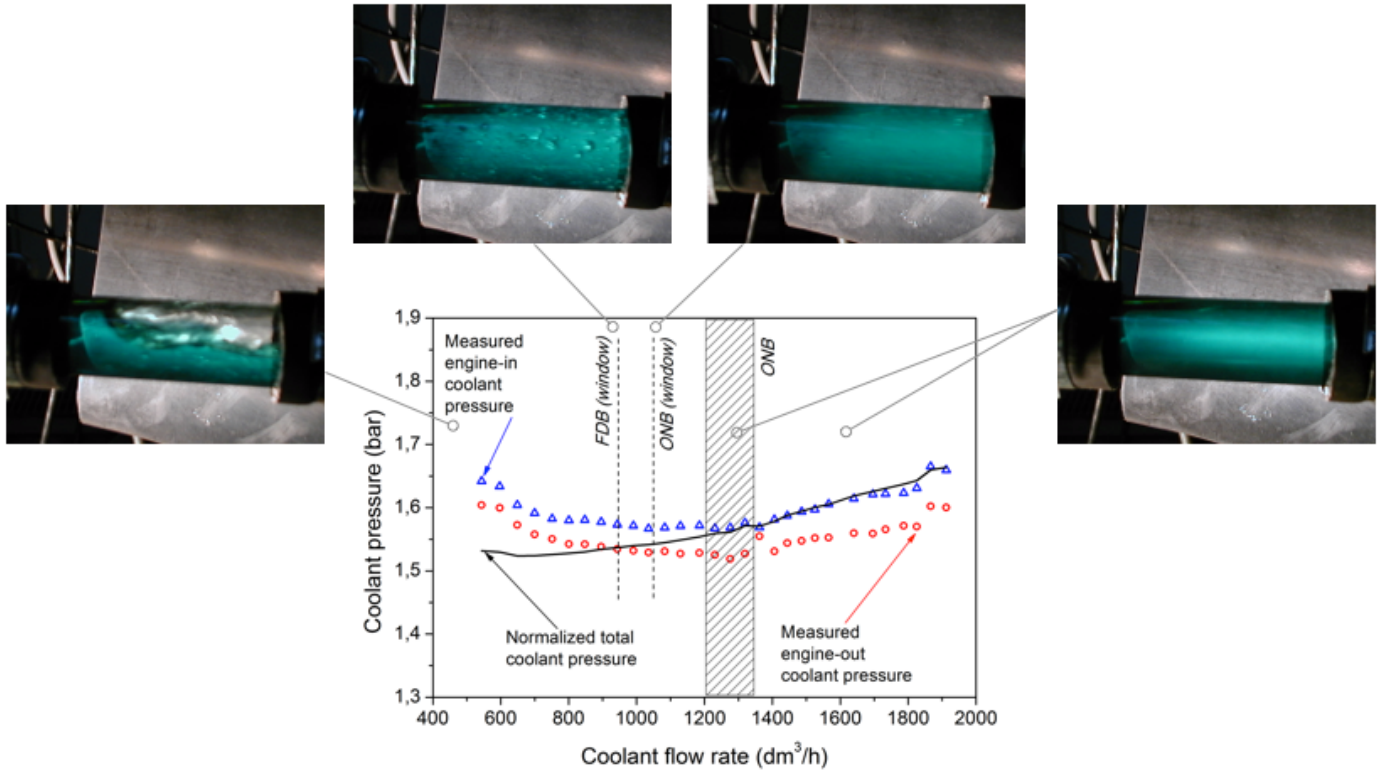


Fig. 8 Comparison of coolant pressure owing to the sum of coolant expansion and pump head contributions and coolant pressure measured at engine inlet and engine outlet. Pictures of the coolant flow through the transparent window are also shown.

225

226

227 **3.2 Coolant temperature**

228

229

230

231

232

233

234

235

236

237

Another hint of the presence of nucleate boiling can be found in the increase of coolant temperature from engine inlet to engine outlet (Fig. 9). In fact, if the heat transfer regime is single-phase forced convection, this temperature difference increases almost linearly as the volumetric coolant flow rate is reduced, while the fuel flow rate, engine speed and engine inlet coolant temperature are kept constant. This is due to the fact that coolant density can be considered constant within the temperature range of interest. On the contrary, when nucleate boiling develops, the coolant temperature from inlet to outlet of the engine shows a more rapid increase as the volumetric coolant flow rate is reduced. In this case, in fact, the presence of bubbles causes a significant decrease in coolant density. More details can be found in [10].

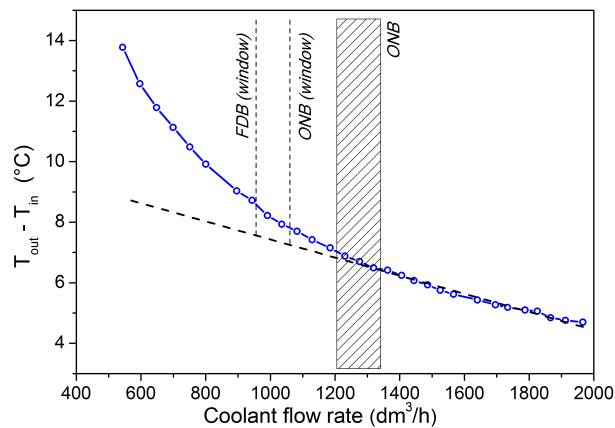


Fig. 9 Difference between coolant temperature at engine outlet and at engine inlet as a function of volumetric coolant flow rate. Dashed area indicates the Onset of Nucleate Boiling (ONB). Operational condition: 2000 rpm, bmep=2 bar.

238

239 3.3 Wall temperature

240 While coolant pressure and engine-in engine-out temperature difference can be
 241 explained in terms of engine behavior in the whole, wall temperatures are local values, which
 242 can be interpreted only by taking into account the characteristics of the single cylinders. The
 243 single cylinders differ in terms of thermal performance for two main reasons: differences in
 244 coolant flow rate distribution and differences in cylinder coolant inlet temperature. Cylinder
 245 4, the left-most one in Fig. 3, is cooled by a smaller coolant flow rate at a lower temperature;
 246 the subsequent cylinders are cooled by an increasing coolant flow rate, which comes partly
 247 from the head of the previous cylinder, and partly from “fresh” coolant rising from the
 248 cylinder block. In addition, there is a further diversity due to the different contribution of
 249 radiation and natural convection to the surrounding ambient. External cylinders (no. 4 and no.
 250 1, Fig 3) have a much larger heat exchange surface than inner cylinders no. 2 and no. 3. For
 251 the engine used in the reported tests, this surface was estimated to be about 35% of the whole
 252 engine external surface for cylinders no. 4 and no. 1 and about 15% for cylinders no. 2 and
 253 no. 3. However, as the free convection and radiation contributions are small, the coolant must
 254 remove a fraction of the whole engine heat transfer for each cylinder, which is only slightly
 255 different: it was estimated at 0.26 for cylinders no. 2 and no. 3 and 0.24 for cylinders no. 1
 256 and no. 4.

257 Data of coolant flow rate distribution among the different cylinders were available from
258 industry confidential reports in the framework of the cooperative research project
259 PON01_01517, CUP: B21H11000400005, with financial support of the European
260 Commission. On the base of these data, a model of the cooling system of an ICE that predicts
261 dynamically the onset of the nucleate boiling phenomenon [10] was used. Inputs of the model
262 are engine speed, fuel flow rate, coolant pressure and temperature at the engine inlet and
263 coolant volumetric flow rate. The model provides engine outlet coolant temperature, spatial
264 averaged metal temperature and the amount of heat exchange area that operates under
265 nucleate boiling conditions. Even though the model [10] was developed for the whole engine,
266 it was used, in this case, to predict the average wall temperature, the cylinder-out coolant
267 temperature and the presence and intensity of nucleate boiling for each cylinder. The
268 *NB_index* is the metrics used to quantify the intensity of nucleate boiling and is defined as:

269

$$NB_index = \frac{(q_w - q_{ONB})}{q_{ONB}} \quad (1)$$

270

271 where q_w is the actual thermal flux and q_{ONB} is the thermal flux required for the onset of
272 nucleate boiling.

273 For cylinder no. 4 the inlet coolant temperature was the engine-in coolant temperature;
274 for the subsequent cylinders the inlet temperature was computed as a mass-weighted average
275 of the temperature of the coolant coming from the previous cylinder and of the temperature of
276 the coolant coming up in the cylinder block, which was assumed still equal to the engine-inlet
277 one. Finally the engine-out coolant temperature derives from the mixing of the coolant
278 coming from the head of cylinder no. 1 and the coolant coming up from the right-most
279 passages of cylinder no.1 (Fig. 3). The simulated working conditions are: total engine-in
280 coolant flow rate 1230 dm³/h; engine-in coolant temperature 85 °C; 2 bar bmep; engine speed
281 2000 rpm.

282 The simulation results are reported in Figure 10. Cylinder inlet temperature increases
283 from the engine-in temperature of cylinder 4 (85 °C) to 89, 90, 90 °C at inlet of cylinders 3, 2
284 and 1 respectively. The predicted cylinder-out temperature is almost constant for the different
285 cylinders (93-94 °C). The predicted engine-out temperature is 90 °C, which is in good
286 agreement with the experimental value (92 °C). As a consequence of coolant temperature and
287 coolant flow rate, which steadily increases from cylinder 4 to cylinder 1, the highest wall
288 temperature is predicted in cylinder 2; wall temperature in cylinders 1 and 3 is only 1-2 °C

289 lower, while the temperature of cylinder 4 is significantly lower (6 °C). Cylinder 2 is also the
 290 one which presents nucleate boiling ($NB_index > 0$), while for cylinders 1, 3 and 4 the model
 291 predicts the absence of nucleate boiling ($NB_index < 0$).

292

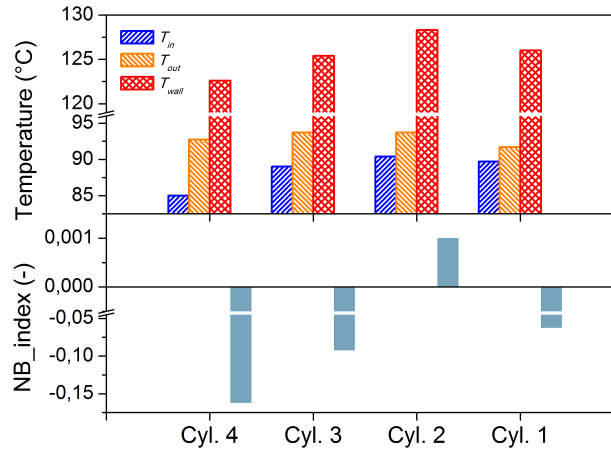


Fig. 10. Predicted values of coolant inlet temperature, coolant outlet temperature, average wall temperature and intensity of nucleate boiling (NB_index) for the different cylinders and for the whole engine. Operational condition: 2000 rpm, bmep=2 bar, 1306 dm³/h coolant flow rate.

293

294 Figure 11 shows measured head temperatures evolution at exhaust and intake valve
 295 bridge locations for an operating condition of 2000 rpm and 2 bar bmep, while the coolant
 296 flow rate ranges from 1900 dm³/h to 500 dm³/h. Model results and experimental data agree,
 297 to indicate that the cylinder 4 is significantly colder than cylinders 1,2 and 3. The difference
 298 in average wall temperature predicted by the model is obviously amplified in the
 299 experimental exhaust valve bridge temperatures, which are the highest in the engine.

300 The wall temperature experimental data can also be used to identify the ONB. It was
 301 shown in [10] that the thermal power transferred from the hot gases to the engine wall can be
 302 expressed as $\dot{Q}_g = cN^{n_1}\dot{m}_c^{n_2}\dot{m}_f^n$ where c , n , n_1 and n_2 are constants and \dot{m}_c , \dot{m}_f and N are
 303 coolant mass flow rate, fuel mass flow rate and engine speed, respectively. Therefore, for
 304 constant engine speed and fuel flow rate, $\dot{Q}_g \propto \dot{m}_c^{n_2}$ where n_2 was estimated at 0.15 for the
 305 engine used for the reported tests. Under single phase forced convection conditions, the

306 thermal power transferred from the engine wall to the coolant is $\dot{Q}_c = hA(T_w - T_c)$ where T_c is
 307 the coolant average temperature, T_w is the average wall temperature, A is exchange area and
 308 the heat transfer coefficient is $h \propto \dot{m}_c^{0.8}$. It was also shown in [10], that, in the presence of
 309 single phase forced convection, the difference between engine-out and engine-in coolant
 310 temperature increases linearly as the coolant volumetric flow rate diminishes (Fig. 9);
 311 therefore, if the engine-in coolant temperature is kept constant, as in present case, this holds
 312 also for the average coolant temperature: $T_c \propto \dot{m}_c$. Under steady-state conditions, $\dot{Q}_g = \dot{Q}_c$
 313 and, therefore, $T_w \propto \dot{m}_c^{-0.65} - \dot{m}_c$. For the values of the involved constants, it results that the
 314 first term is one order of magnitude lower than the second one for coolant flow rates greater
 315 than about 0.37 kg/s (1300 dm³/h), so that, if the heat transfer regime is single phase forced
 316 convection:

$$T_w = const - K \cdot \dot{m}_c \quad (2)$$

318
 319 When ONB occurs, the coolant temperature increases more than linearly as the coolant flow
 320 rate diminishes (Fig. 9) and this also happens for the wall temperature.

321 Figure 12 shows that the nucleate boiling occurs first in cylinder 2, for a coolant flow
 322 rate of about 1200-1300 dm³/h. This value is in agreement with the ones resulting from the
 323 analysis of coolant pressure and temperature data for the whole engine (Fig. 8 and 9). Figure
 324 12 also shows that, as the coolant flow rate further diminishes the nucleate boiling occurs in
 325 the order in cylinders 3, 1 and 4. This is in agreement with results of the simplified analysis
 326 carried out with the zero-dimensional model [10] shown in Fig. 10.

327

328

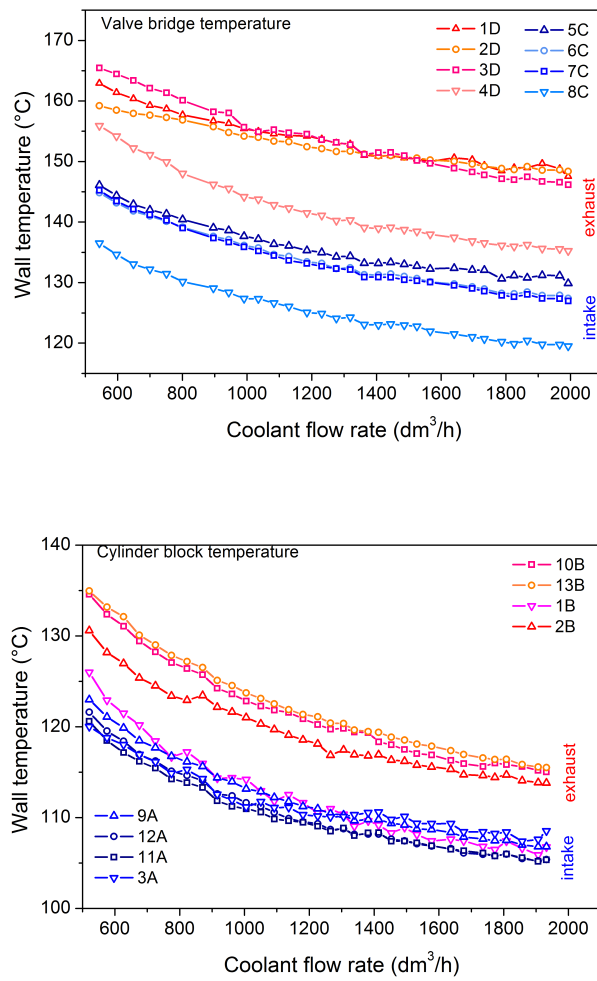


Fig. 11. Wall temperature recorded in the engine head (top) and in the cylinder block (bottom), as a function of volumetric coolant flow rate. Numbers in the legend refer to the thermocouples designation in Fig. 3. Operational condition: 2000 rpm, bmep=2 bar

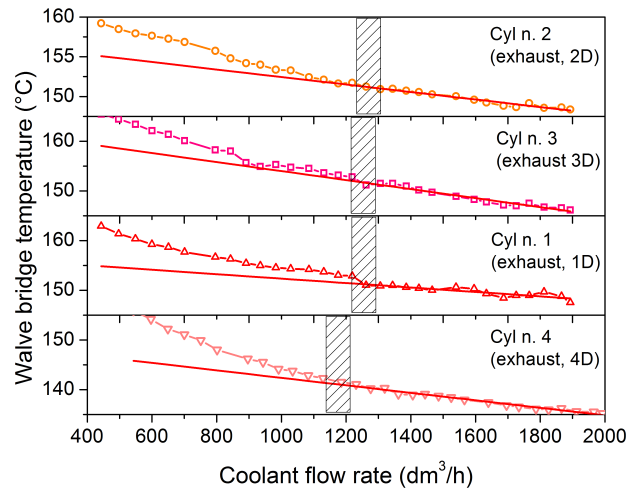


Fig. 12. Wall temperature recorded in the engine head as a function of volumetric coolant flow rate. Dashed area indicates the Onset of Nucleate Boiling (ONB). Operational condition: 2000 rpm, bmep=2 bar.

330

331 **3.4 Nucleate Boiling Area**

332 The fraction of cooling circuit, which operates under nucleate boiling, cannot be
 333 obtained directly from experimental data. The model which predicts the onset of the nucleate
 334 boiling [10] was therefore used. Figure 13 shows the ratio of this quantity to the total heat
 335 exchange area and the corresponding value of *NB_index*. The results of the model are well in
 336 agreement with the conclusions of the experimental observation. The calculated Nucleate
 337 Boiling Area is, in fact, zero for coolant flow rates higher than about 1250 dm³/h and
 338 increases as the coolant flow rate is reduced below this value.

339

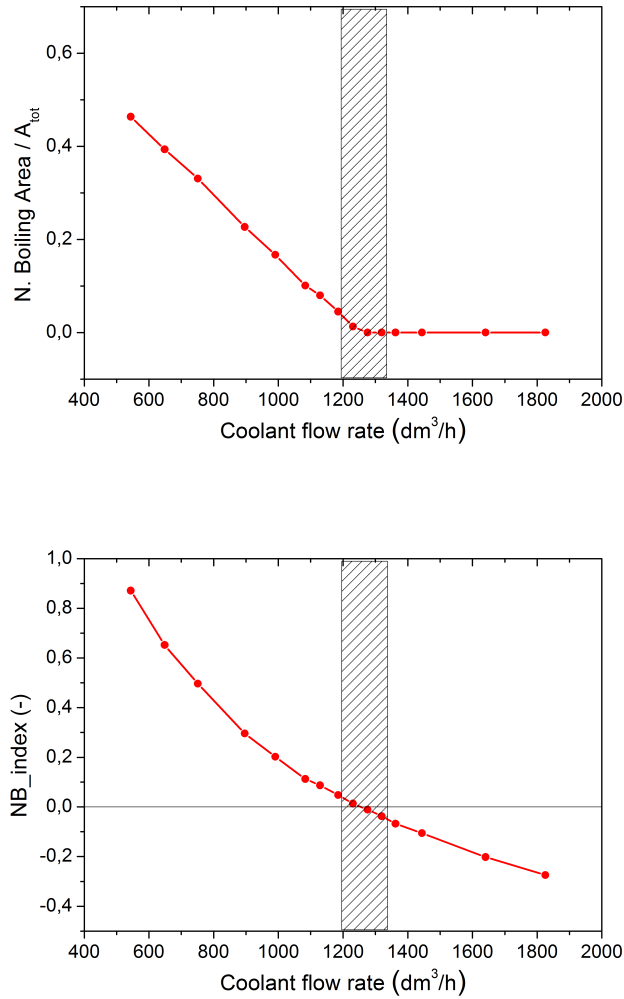


Fig. 13. Fraction of cooling circuit area which operates in nucleate boiling regime (top) and *NB_index* (bottom) as a function of coolant flow rate.

340 **4. SUMMARY AND CONCLUSIONS**

341 Several experimental campaigns were carried out to investigate the onset of nucleate
 342 boiling condition: the coolant flow rate was varied in a sequence of steady state conditions,
 343 while engine speed, bmep and inlet coolant temperature were maintained constant. Attention
 344 was paid to coolant pressure and temperature behavior and to wall temperature, which result
 345 from coolant flow rate variations. The indications of other quantities like the coolant pressure
 346 pulsations or the engine-in engine-out volumetric flow rate comparison are not clear enough
 347 when a standard closed radiator expansion tank is used.

348 The trends of these quantities provide clear hints to identify the coolant flow rate range
349 where the onset of nucleate boiling occurs, which are in good agreement among them.
350 However, it appears rather problematic to assess the occurrence of nucleate boiling from one
351 single measurement of one or more of these quantities; only the analysis of their trend seems
352 to make it possible. This is especially true when engine operating conditions are continuously
353 varying or when the measurements have to be taken on board a vehicle. In addition, a
354 warning must be flagged on the repeatability of the nucleate boiling phenomenon in the
355 engine under real operating conditions. A difference in the initial coolant level within the
356 cooling circuit or an air leakage of the radiator cap would cause a significant discrepancy in
357 the operating pressure of the cooling circuit and, consequently, an important variation in the
358 tendency to the onset of nucleate boiling.

359 The use of a lumped parameter dynamic model of the cooling system, which
360 incorporates the description of the nucleate boiling regime [10], seems, on the contrary,
361 adequate to determine whether a given engine operating condition causes nucleate boiling or
362 not and is therefore suitable for the on-board identification of the heat transfer mechanism.

363

364

365 **5. ACKNOWLEDGEMENTS**

366 The investigation was funded by the Italian Ministry of University and Research under
367 the project PON01_01517, CUP: B21H11000400005, with financial support of the European
368 Commission.

369 Technical support was provided by Mr. Ernesto Ramundo, whose cooperation is
370 gratefully acknowledged.

371

372

373 **REFERENCES**

374 1. Will, F., Boretti, A. A new method to warm up lubricating oil to improve the fuel
375 efficiency during cold start. *SAE Int. J. Engines* 2011; 4(1):175-187. DOI:
376 10.4271/2011-01-0318.

377 2. Will, F. Fuel conservation and emission reduction through novel waste heat recovery
378 for internal combustion engines. *Fuel* 2012; 102:247–55.
379 DOI:10.1016/j.fuel.2012.06.044.

- 380 3. Trapy, J.D., Damiral, P. An investigation of lubricating system warm-up for the
381 improvement of cold start efficiency and emissions of SI automotive engines. SAE
382 technical paper 902089, 1990. DOI:10.4271/902089.
- 383 4. Samhaber, C., Wimmer, A., Loibner, E. Modeling of engine warm-up with integration
384 of vehicle and engine cycle simulation. SAE technical paper 2001-01-1697, 2001; 55-
385 62.
- 386 5. Brace, C.J., Burnham-Slipper, H., Wijetunge, R.S., Vaughan, N.D., Wright, K.,
387 Blight, D. Integrated Cooling System for Passenger Vehicles. SAE Technical Paper
388 2001-01-1248, 2001. DOI: 10.4271/2001-01-1248.
- 389 6. Ap, N. and Golm, N. New Concept of Engine Cooling System (Newcool). SAE
390 Technical Paper 971775, 1997. DOI:10.4271/971775.
- 391 7. Brace CJ, Hawley G, Akehurst S, Piddock M, Pegg I. Cooling system improvements
392 – assessing the effects on emissions and fuel economy. Proc Inst Mech Eng Part D: J
393 Automob Eng 2008; 222(4):579–91. DOI: 10.1243/09544070JAUTO685.
- 394 8. Bent E, Shayler P, La Rocca A. The effectiveness of stop–start and thermal
395 management measures to improve fuel economy. Presented at VTMS 11, Coventry;
396 2013.
- 397 9. Gardiner R, Zhao C, Addison J, Shayler PJ. The effects of thermal state changes on
398 friction during the warm up of a spark ignition engine. Presented at VTMS 11,
399 Coventry, UK; 2013.
- 400 10. S. Bova, T. Castiglione, R. Piccione and F. Pizzonia , A Dynamic Nucleate-Boiling
401 model for CO₂ reduction in Internal Combustion Engines, Applied Energy, 143
402 (2015), pp. 271-282.
- 403 11. M. Amelio, F. Barbara, S. Bova, P. Oliva, Experimental Investigation on an ICE
404 Cooling System under Nucleate Boiling Conditions, SAE paper n. 2001 01 1795,
405 Proceedings of SETC, Pisa, 2001, pp. 697-703.
- 406 12. Rohsenow, W.M. A method of correlating heat transfer data for surface boiling of
407 liquids, J. Heat Transfer Trans. ASME 1952; 74:969–976.
- 408 13. Engelberg-Forster, K. and Greif, R. Heat transfer to a boiling liquid – mechanism and
409 correlations, J. Heat Transfer Trans. ASME 1959; 81:43–53.
- 410 14. Foster, H.K. and Zuber, N. Dynamics of Vapor Bubbles and Boiling Heat Transfer.
411 AIChE Journal 1955; 1(4):531-535. DOI:10.1002/aic.690010425.
- 412 15. Pretschner, M. and Ap, N.S. Nucleate Boiling Engine Cooling System – Vehicle Study,
413 SAE Technical Paper 931132, 1993. DOI:10.4271/931132.
- 414 16. Collier, J. and Thome, R. Convective Boiling and Condensation, Oxford University
415 Press, New York, 1994.
- 416 17. Sanna, A. , Hutter, C., Kenning, D.B.R., Karayiannis, T.G., Sefiane, K., Nelson, R.A.
417 Numerical investigation of nucleate boiling heat transfer on thin substrates, Int. J.
418 Heat Mass Tran. 2014; 76:45–64. DOI:10.1016/j.ijheatmasstransfer.2014.04.026.

- 419 18. Johnson, T. Vehicular Emissions in Review. SAE Int. J. Engines 2012; 5(2):216-234.
420 DOI:10.4271/2012-01-0368.
- 421 19. Bishop, J., Martin, N., Boies, A. Cost-effectiveness of alternative powertrains for
422 reduced energy use and CO₂ emissions in passenger vehicles. Appl. Energ. 2014; 124:
423 44-61.
- 424 20. Silva, C., Ross, M., Farias, T. Analysis and simulation of “low-cost” strategies to
425 reduce fuel consumption and emissions in conventional gasoline light-duty vehicles.
426 Energ.Convers.Manage. 2009; 50(2):215–222. DOI:10.1016/j.enconman.2008.09.046.
- 427 21. Bova, S., Piccione, R., Durante D., Perrussio, M. Experimental Analysis of the After-
428 Boiling Phenomenon in a Small I.C.E. SAE Technical Paper 2004-32-0091, 2004.
429 DOI:10.4271/2004-32-0091.
- 430 22. Pizzonia, F., Castiglione, T., Bova, S. A Robust Model Predictive Control for
431 Efficient Thermal Management of Internal Combustion Engines, submitted to Applied
432 Energy.
- 433
- 434

435

FIGURES CAPTIONS

436 **Fig.1** Schematic of the test rig.

437 **Fig.2** Schematic of the cooling circuit.

438 **Fig.3** Thermocouples location in the engine metal and cylinder number identification.

439 **Fig.4** Influence of the coolant temperature on coolant pressure within the sealed circuit at
440 switched-off engine and pump.

441 **Fig.5** Pump and circuit characteristics.

442 **Fig.6** Fractions of pump head which develops at pump delivery and at pump suction side.

443 **Fig.7** Coolant pressure owing to the sum of coolant expansion and pump head contributions
444 as a function of volumetric coolant flow rate.

445 **Fig.8** Comparison of coolant pressure owing to the sum of coolant expansion and pump head
446 contributions and coolant pressure measured at engine inlet and engine outlet. Pictures of the
447 coolant flow through the transparent window are also shown.

448 **Fig.9** Difference between coolant temperature at engine outlet and at engine inlet as a
449 function of volumetric coolant flow rate. Dashed area indicates the Onset of Nucleate Boiling
450 (ONB). Operational condition: 2000 rpm, bmep=2 bar.

451 **Fig.10** Predicted values of coolant inlet temperature, coolant outlet temperature, average wall
452 temperature and intensity of nucleate boiling (NB_index) for the different cylinders and for
453 the whole engine. Operational condition: 2000 rpm, bmep=2 bar, 1306 dm³/h coolant flow
454 rate.

455 **Fig.11** Wall temperature recorded in the engine head (top) and in the cylinder block (bottom),
456 as a function of volumetric coolant flow rate. Numbers in the legend refer to the
457 thermocouples designation in Fig. 3. Operational condition: 2000 rpm, bmep=2 bar.

458 **Fig.12** Wall temperature recorded in the engine head as a function of volumetric coolant flow
459 rate. Dashed area indicates the Onset of Nucleate Boiling (ONB). Operational condition:
460 2000 rpm, bmep=2 bar.

461 **Fig.13** Fraction of cooling circuit area which operates in nucleate boiling regime (top) and
462 *NB_index* (bottom) as a function of coolant flow rate..

463

464

TABLE CAPTIONS

465 **Table 1** Main measurement devices specifications.

466 **Table 2** Summary of the experimental tests.

467